Nanoscale Res Lett (2010) 5:1177–1181
DOI 10.1007/s11671-010-9622-1

NANO EXPRESS

# Tin Oxide Nanorod Array-Based Electrochemical Hydrogen Peroxide Biosensor

**Jinping Liu · Yuanyuan Li · Xintang Huang · Zhihong Zhu**

Received: 3 December 2009 / Accepted: 26 April 2010 / Published online: 11 May 2010


**Abstract** $SnO_2$ nanorod array grown directly on alloy substrate has been employed as the working electrode of $H_2O_2$ biosensor. Single-crystalline $SnO_2$ nanorods provide not only low isoelectric point and enough void spaces for facile horseradish peroxidase (HRP) immobilization but also numerous conductive channels for electron transport to and from current collector; thus, leading to direct electrochemistry of HRP. The nanorod array-based biosensor demonstrates high $H_2O_2$ sensing performance in terms of excellent sensitivity (379 μA $mM^{-1}$ $cm^{-2}$), low detection limit (0.2 μM) and high selectivity with the apparent Michaelis–Menten constant estimated to be as small as 33.9 μM. Our work further demonstrates the advantages of ordered array architecture in electrochemical device application and sheds light on the construction of other high-performance enzymatic biosensors.

**Keywords** Nanostructure · $SnO_2$ · Nanorod array · Biosensor

## Introduction

The determination of hydrogen peroxide ($H_2O_2$) has attracted great attention because $H_2O_2$ plays an important role in food industry, clinical diagnosis and environmental monitoring [1]. The $H_2O_2$ detection is also of special interest in terms of tracking many biological targets such as glucose and lactose. Among various analytical techniques, electrochemical enzyme biosensor is most tempting due to its simplicity, high selectivity of the biological recognition elements and high sensitivity of electrochemical transduction process [2–4]. To achieve high biosensor performance, it is very necessary to fabricate novel electrode materials for both effective immobilization of enzyme (without losing the enzymatic bioactivity) and fast electron transport from enzyme to metallic electrode [5–7]. Over the past decades, nanostructured materials have emerged as promising electrode material candidates because of their regular structure, high active surface area for protein binding and good chemical and thermal stability [8]. However, most electrodes using nanostructures for the direct determination of biomolecules such as $H_2O_2$ still have several problems unsolved. For example, the fabrication of electrodes conventionally involves casting nanostructure powders with insulating polymer binders onto current collector [1–4, 8]. In this case, the response time and sensitivity of biosensor may be significantly limited by the electron transport through numerous interparticle contact areas. In addition, the sensing based on biomolecule oxidation is always at very high working potential, at which the interference from electroactive substrates coexisting in the sample media cannot be avoided.

Very recently, a perfect electrode architecture consisting of single-crystalline (ZnO, $TiO_2$, Si, etc.) nanorod/nanowire/nanotube arrays grown directly on metal substrate was proposed to address the above impasse [5–7, 9]. These aligned one-dimensional (1D) nanostructures not only provide large-area scaffolds for enzyme immobilization but also direct channels for electron transport from redox enzymes to current collector. In several cases, this

J. Liu (✉) · Y. Li · X. Huang · Z. Zhu
Department of Physics, Central China Normal University, Wuhan 430079, People's Republic of China
e-mail: liujp@phy.ccnu.edu.cn

Y. Li
State Key Laboratory of Advanced Technology for Materials Synthesis and Processing, Wuhan University of Technology, Wuhan 430070, People's Republic of China

architecture leads to the realization of enzymatic direct electrochemistry that typically operates at negative potentials [9]. Tin oxide ($SnO_2$), a wide bandgap semiconductor, is well known for its excellent gas sensitivity [10, 11] and its use in fabricating transparent conductive glasses [12]. $SnO_2$ nanowires and their arrays have also been investigated for photoluminescence [13], lasing [14], field emission [15], transistors, solar cells [16] and lithium ion batteries [10, 17]. In particular, $SnO_2$ is biocompatible [18–20], cheaper than Si, more stable than ZnO in physiological environment and more conductive than $TiO_2$ [17]. Despite these, there is no report yet on applying $SnO_2$ nanorod/nanowire arrays in electrochemical biosensors.

Herein, we present the use of direct-grown $SnO_2$ nanorod arrays as a new platform for biosensing at low potential (-0.45 V), taking $H_2O_2$ detection as a case study. The low isoelectric point of $SnO_2$ (4.0 $\sim$ 5.0) facilitates the homogeneous immobilization of horseradish peroxidase (HRP; isoelectric point: 7.2) through electrostatic interaction. The facile HRP loading combined with ordered array architecture endows the constructed biosensor with very low detection limit and high sensitivity.

## Experimental

$SnO_2$ nanorod arrays were synthesized by a facile hydrothermal method [17]. Typically, a transparent solution of $Sn(OH)_6^{2-}$ was first prepared by mixing 1.17 g $SnCl_4{\cdot}5H_2O$ and 2.0 g NaOH; it was then transferred into a Teflon-lined autoclave (80 ml) with a Fe-based alloy substrate present, which was subsequently heated to 200°C for 24 h. After the reaction, the obtained $SnO_2$ arrays on alloy substrate further underwent an annealing treatment at 400°C for 2 h in Ar gas. The product was characterized using powder X-ray diffraction (XRD) (Bruker D-8 Avance), transmission electron microscopy (TEM) (JEM-2010FEF, 200 kV), scanning electron microscopy (SEM) (JSM-6700F, 5.0 kV), and Raman spectroscope (Witech CRM 200, 532 nm).

For a typical process of protein immobilization, 10 μl HRP solution (15 mg $ml^{-1}$, 0.01 M PBS, pH 7.0) was dropped onto 0.75 × 0.75 $cm^2$ $SnO_2$ array alloy electrode surface. After the evaporation of water, the electrode was stored at 4°C. Prior to the measurement, the electrode was rinsed in 0.01 M PBS to remove the unimmobilized HRP, a 5 μl 0.5 w% Nafion solution was further introduced to form a tight membrane on the surface. The electrochemical properties were examined with a electrochemical workstation (CHI) utilizing a conventional three-electrode system, which consists of a $SnO_2$ array on alloy as the working electrode, a Pt wire as the counter electrode, and a saturated calomel electrode (SCE) as the reference. The electrolyte was 0.1 M pH 7.0 $N_2$-saturated PBS solution. A continuous stream of $N_2$ was introduced into the cell above the liquid surface to maintain an inert atmosphere over the testing solution.

## Results and Discussion

Figure 1a shows the typical SEM image of $SnO_2$ nanorod arrays. The nanorods are grown uniformly on alloy foil with average diameter of 20 nm. The highly single crystalline structure of $SnO_2$ is confirmed by HRTEM, as displayed in Fig. 2b. In Fig. 2b, the spacing of the lattice fringes is 3.32 Å, which can be indexed as (110) of rutile $SnO_2$. Therefore, the nanorods grow along the *c* axis with four side surfaces enclosed by {110} planes. The composition of the nanorod array is further evidenced by XRD analysis and Raman spectrum (Fig. 1c and d). Three fundamental Raman scattering peaks at 478, 631 and 774 $cm^{-1}$ are clearly observed. These peak positions are in good agreement with those reported previously [15] and could be assigned to $E_g$, $A_{1g}$, and $B_{2g}$ acoustic vibration modes, respectively. The void spaces between neighboring nanorods provide large surface area for protein access and immobilization.

Figure 2 illustrates three cyclic voltammograms (CVs) of the HRP-loaded array at sweep rate of 100, 300 and 500 mV $s^{-1}$, respectively. It is clear that all the CV traces exhibit the obvious reduction peak of HRP by the $Fe^{3+}$/$Fe^{2+}$ conversion reaction (−0.47 V) [21]. Comparative experiments also indicated that no voltammeric redox peaks were detected at both HRP/alloy electrode and pristine array/alloy electrode. Thus, $SnO_2$ nanorod array can retain HRP bioactivity and plays an important role in direct electron transfer between the HRP enzyme and alloy substrate. We further investigated the electrocatalytic reduction of HRP on nanorod array electrode toward $H_2O_2$ by CV (Fig. 3a). With the addition of $H_2O_2$ to the PBS solution, the reduction current increases dramatically with the decrease in the oxidation current, which is attributed to the presence of more oxidative HRP($HRP_{ox}$) arising from the reaction between $HRP_{red}$ and $H_2O_2$ [18, 21]. The more $H_2O_2$ added, the larger the reduction current achieved, indicating the HRP modified on the nanorod array can act as an efficient catalyst to the reduction of $H_2O_2$. It should be noticed that the optimum immobilization concentration of HRP is 15 mg $ml^{-1}$, as demonstrated in Fig. 3b. When either high or low HRP concentrations are used, there are smaller reduction currents at −0.47 V in the CV. It is believed that under optimized condition the nanorods in the array are able to have direct contact with adsorbed HRP. However, further increase in the HRP concentration results in a HRP layer

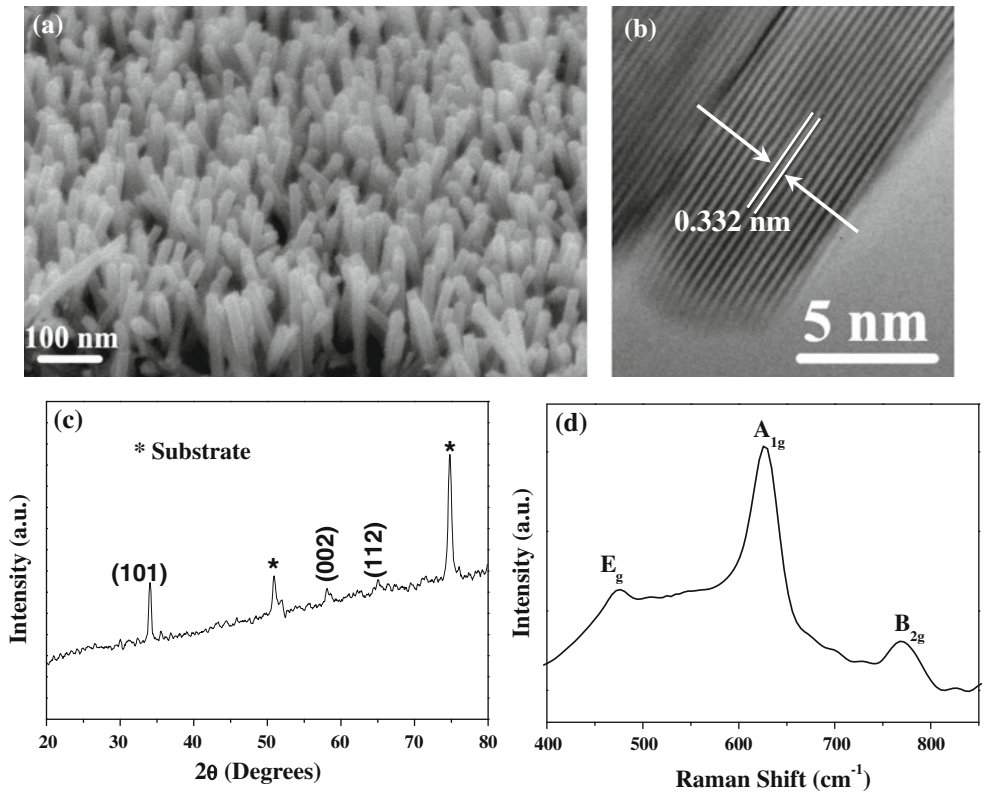


**Fig. 1** **a** Typical SEM image of $SnO_2$ nanorod array. **b** HRTEM image of an individual nanorod. **c** XRD and **d** Raman spectrum of the $SnO_2$ nanorod array

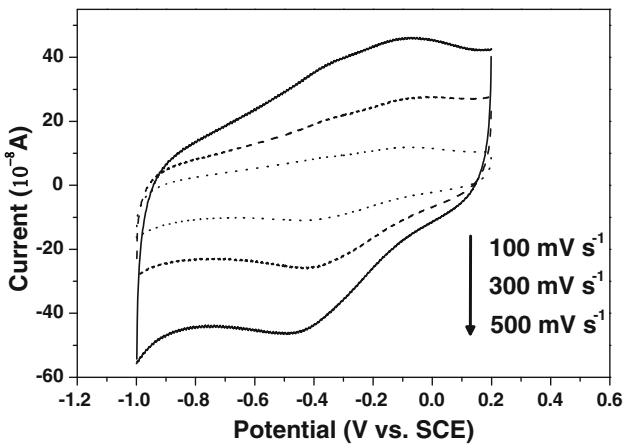


**Fig. 2** CVs of HRP/$SnO_2$ nanorod array electrode in $N_2$-saturated PBS solution at different scan rates

too thick to have the effect of direct electron transfer with the nanostructure electrode surface.

On the basis of the aforementioned results, a biosensor was constructed to quantitatively determine the concentration of $H_2O_2$. Figure 4 shows the calibration curve of the biosensor under the optimized condition. A linear relationship between the catalytic reduction current and $H_2O_2$ concentration is obtained in the range from 0.8 to 35 μM with the linear regression equation as $I(\mu A) = 0.213c$ (μM) + 0.005($r = 0.99$, $n = 16$). The detection limit is estimated to be 0.2 μM at signal-to-noise(S/N) ratio of three. Note that this detection limit is only 1/10 times of that obtained on HRP-$TiO_2$ nanotube-modified electrode [21] and smaller than many other reported results [18, 22–26]. From the slope of the regression equation, the sensitivity of our biosensor can be further determined to be as high as ~379 μA $mM^{-1}$ $cm^{-2}$. This value is even slightly higher than that of the biosensor constructed with nano-sized Au-ZnO (369 μA $mM^{-1}$ $cm^{-2}$) [27]. When the concentration of $H_2O_2$ is more than 35 μM, a catalytic current plateau emerges, which suggests a typical electrocatalytic process with Michaelis–Menten kinetic model. The apparent Michaelis–Menten constant ($K_M^{app}$) can be further calculated from the electrochemical version of the Lineweaver–Burk equation, which provides an indicative of the enzyme-substrate kinetics: $1/I_m = 1/I_{max} + K_M^{app}/(cI_{max})$, where $I_m$ is the steady current after the addition of $H_2O_2$, $c$ is the bulk concentration of $H_2O_2$, and $I_{max}$ is the maximum current measured under the saturated condition [9, 18]. By analyzing the slop and the intercept of the plot of the reciprocals of the current versus $H_2O_2$ concentration (inset in Fig. 4), the $K_M^{app}$ value is calculated as 33.9 μM, which is smaller than some reported $H_2O_2$

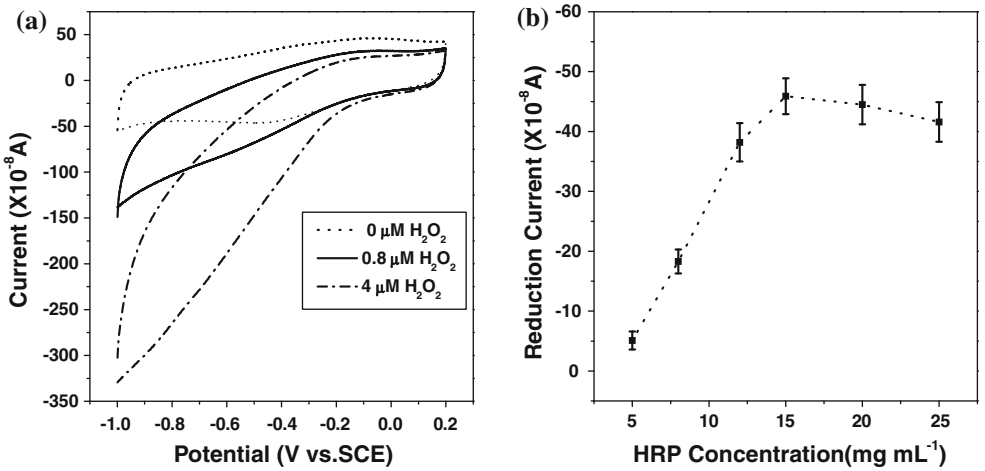


**Fig. 3** **a** CVs of HRP/$SnO_2$ nanorod array electrode in $N_2$-saturated PBS solution containing 0, 0.8 and 4 μM $H_2O_2$, respectively. **b** Effect of HRP dosage on the reduction current responses of the developed enzymatic electrode. Scan rate: 500 mV $s^{-1}$

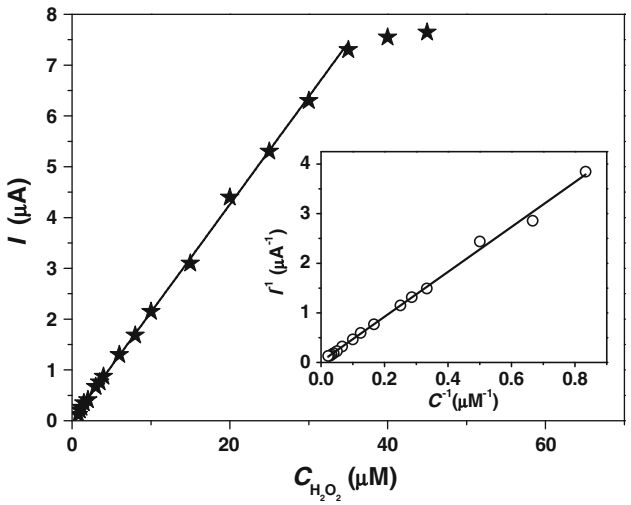


**Fig. 4** Calibration curve for the $SnO_2$ array-based $H_2O_2$ biosensor at −0.47 V. Inset is the corresponding Lineweaver–Burk plot

biosensor [18, 22]. The smaller value indicates the higher affinity of immobilized HRP on the $SnO_2$ nanorod array to $H_2O_2$.

As discussed earlier, array-based biosensor displays excellent analytical performance in terms of detection limit, sensitivity and linear range (see Table 1 for the comparison of detailed analytical performances from biosensors using different substrate materials for enzyme immobilization). This should be attributed to the following two main reasons: First, the geometrical configuration of the nanorod array provides large void spaces for assembling bioactive HRP with high amount; the enzyme assembly is, on the other hand, basically promoted through the electrostatic interaction between HRP and $SnO_2$. Secondly, nanorods are single-crystalline structures without grain boundaries, forming direct conduction channels, a highway for electrons. These are in sharp contrast to the tortuous percolation network of the nanoparticle films. Thus, the nanorod array grown tightly on alloy serves as the "electronic wires" for the electron transferring between the HRP-active sites and the alloy substrate surface.

The detection reproducibility of the developed sensor was also examined by repeated detections of $H_2O_2$. When 4 μM $H_2O_2$ was measured continuously for eight assaying runs, a relative standard deviation (RSD) of 7.5% was obtained. In addition, the storage stability of the HRP-

**Table 1** Comparison of analytical performances of $H_2O_2$ biosensors using different substrate materials for enzyme immobilization

| Substrate materials | Immobilized enzyme | Sensitivity (μA $mM^{-1}$ $cm^{-2}$) | Detection limit (μM) | Reference |
|---|---|---|---|---|
| C- $TiO_2$ nanotube | Hemoglobin (Hb) | 8.57 | 0.92 | 19 |
| Au-$TiO_2$ nanotube | HRP | Not available | 2 | 18 |
| ZnO-C nanowire array | HRP | 237.8 | 0.2 | 9 |
| Au | HRP | 271 | 1.2 | 24 |
| Nanosized ZnO | HRP | 255 | 4.0 | 24 |
| Nanosized Au-ZnO | HRP | 369 | 0.7 | 24 |
| $SnO_2$ nanorod array | HRP | 379 | 0.2 | This work |

modified array electrode was tested by measuring the current responses to 4 μM $H_2O_2$ at intervals of 5 days during one month when the biosensor was stored in the refrigerator at 4°C. It was discovered that the so prepared electrode could retain about 92% electrocatalytic activity to $H_2O_2$ after one month storage. Other advantages of the $SnO_2$ array-based biosensor are the low detection potential (−0.47 V) and high HRP enzyme selectivity, which could eliminate the interference of other substrates such as citric acid, ascorbic acid, sucrose and glucose [28]. The addition of these common interfering species into the PBS showed negligible influence on $H_2O_2$ determination.

## Conclusions

In sum, a novel biosensor based on immobilization of HRP on $SnO_2$ nanorod array electrode has been developed. The three-dimensional (3D) array architecture provides a favorable microenvironment around HRP to retain the enzymatic bioactivity, while the vertically aligned single-crystalline $SnO_2$ nanorods ensure numerous direct electron transport channels to electrode. Accordingly, the HRP/array electrode is demonstrated for determination of $H_2O_2$ at an applied potential of −0.47 V with excellent sensitivity, low detection limit and high selectivity. 3D microelectrode fabricated by direct growth offers a relatively straightforward means to produce biosensors on a mass scale and represents a useful platform for electroanalysis applications.

**Acknowledgments** This work was financially supported by National Natural Science Foundation of China (No. 50872039; 50802032).



## References

1. L.Wang, E.K. Wang, Electrochem. Commun. **6**, 225 (2004)
2. W. Sun, X.Q. Li, Y. Wang, R.J. Zhao, K. Jiao, Electrochim. Acta **124**, 494 (2007)
3. W.J. Zhang, G.X. Li, Anal. Sci. **20**, 603 (2004)
4. E.E. Ferapontova, V.G. Grigorenko, A.M. Egorov, T. Borcher, T. Ruzgas, L. Gorton, Biosens. Bioelectron. **16**, 147 (2001)
5. A. Wei, X.W. Sun, J.X. Wang, Y. Lei, X.P. Cai, C.M. Li, Z.L. Dong, W. Huang, Appl. Phys. Lett. **89**, 123902 (2006)
6. J.X. Wang, X.W. Sun, A. Wei, Y. Lei, X.P. Cai, C.M. Li, Z.L. Dong, Appl. Phys. Lett. **4**, 88 (2006)
7. W.W. Chen, H. Yao, C.H. Tzang, J.J. Zhu, M.S. Yang, S.T. Lee, Appl. Phys. Lett. **87**, 213104 (2006)
8. S.P. Singh, S.K. Arya, P. Pandey, B.D. Malhotra, S. Saha, K. Sreenivas, V. Gupta, Appl. Phys. Lett. **91**, 063901 (2007)
9. J.P. Liu, C.X. Guo, C.M. Li, Y.Y. Li, Q.B. Chi, X.T. Huang, L. Liao, T. Yu, Electrochem. Commun. **11**, 202 (2009)
10. N. Du, H. Zhang, J.X. Yu, P. Wu, C.X. Zhai, Y.F. Xu, J.Z. Wang, D.R. Yang, Chem. Mater. **21**, 5264 (2009)
11. Y.J. Chen, X.Y. Xue, Y.G. Wang, T.H. Wang, Appl. Phys. Lett. **87**, 233503 (2005)
12. G.Z. Shen, P.C. Chen, K. Ryu, C.W. Zhou, J. Mater. Chem. **19**, 828 (2009)
13. R. Chen, G.Z. Xing, J. Gao, Z. Zhang, T. Wu, H.D. Sun, Appl. Phys. Lett. **95**, 061908 (2009)
14. C.W. Cheng, B. Liu, H.Y. Yang, W.W. Zhou, L. Sun, R. Chen, S.F. Yu, J.X. Zhang, H. Gong, H.D. Sun, H.J. Fan, ACS Nano. **3**, 3069 (2009)
15. Z. Zhang, J. Gao, L.M. Wong, J.G. Tao, L. Liao, Z. Zheng, G.Z. Xing, H.Y. Peng, T. Yu, Z.X. Shen, C.H.A. Huan, S.J. Wang, T. Wu, Nanotechnology **20**, 135605 (2009)
16. K. Tennakone, G.R.R.A. Kumara, I.R.M. Kottegoda, V.P.S. Perera, Chem. Commun. 15 (1999)
17. J.P. Liu, Y.Y. Li, X.T. Huang, R.M. Ding, Y.Y. Hu, J. Jiang, L. Liao, J. Mater. Chem. **19**, 1859 (2009)
18. N.Q. Jia, J. Xu, M.H. Sun, Z.Y. Jiang, Anal. Lett. **38**, 1237 (2005)
19. A.A. Ansari, A. Kaushik, P.R. Solanki, B.D. Malhotra, Electroanalysis **21**, 965 (2009)
20. J.J. Feng, J.T. Zhu, J.J. Xu, H.Y. Chen, J. Nanosci. Nanotechnol. **9**, 2290 (2009)
21. A.K.M. Kafi, G.S. Wu, A.C. Chen, Biosens. Bioelectron. **24**, 566 (2008)
22. C.X. Guo, F.P. Hu, C.M. Li, P.K. Shen, Biosens. Bioelectron. **24**, 819 (2008)
23. T. Tangkuaram, C. Katikawong, W. Veerasai, Biosens. Bioelectron. **22**, 2071 (2007)
24. L. Zhang, Q. Zhang, J.H. Li, Adv. Funct. Mater. **17**, 1958 (2007)
25. K. Schachl, H. Alemu, K. Kalcher, J. Jezkova, I. Vancara, K. Vytras, Analyst **122**, 985 (1997)
26. M. Viticoli, A. Curulli, A. Cusma, S. Kaciulis, S. Nunziante, L. Pandolfi, F. Valentini, G. Padeletti, J. Mater. Sci. Eng. **26**, 947 (2006)
27. Y.W. Zhang, Y. Zhang, H. Wang, B.N. Yan, G.L. Shen, R.Q. Yu, J. Electroanal. Chem. **627**, 9 (2009)
28. C.M. Li, C.S. Cha, Front. Biosci. **9**, 3324 (2004)